

# Interstellar $C_2$ in the Perseus molecular complex: excitation temperature and density of a molecular cloud with anomalous microwave emission.

Susana Iglesias-Groth<sup>1,2\*</sup>

<sup>1</sup> *Instituto de Astrofísica de Canarias, 38200 La Laguna, Tenerife, Canary Islands, Spain*

<sup>2</sup> *Universidad de La Laguna, E-38205 La Laguna, Tenerife, Spain*

Accepted Received In original form

## ABSTRACT

Interstellar absorption lines up to  $J''=10$  in the (2,0) band and up to  $J''=6$  in the (3,0) band of the  $C_2$   $A^1\Pi_u - X^1\Sigma_g^+$  system are detected toward star Cernis 52 (BD+31° 640) in the Perseus molecular complex. The star lies in a reddened line of sight where various experiments have detected anomalous microwave emission spatially correlated with dust thermal emission. The inferred total  $C_2$  column density of  $N(C_2) = (10.5 \pm 0.2) \times 10^{13} \text{ cm}^{-2}$  is well correlated with that of CH as expected from theoretical models and is among the highest reported on translucent clouds with similar extinction. The observed rotational  $C_2$  lines constrain the gas-kinetic temperature  $T$  and the density  $n=n(H)+n(H_2)$  of the intervening cloud to  $T = 40 \pm 10 \text{ K}$  and  $n = 250 \pm 50 \text{ cm}^{-3}$ , respectively. This is the first determination of gas-kinetic temperature and particle density of a cloud with known anomalous microwave emission.

**Key words:** ISM:molecules—ISM:lines and bands—ISM:abundances

## 1 INTRODUCTION

The moderately reddened [E(B-V)=0.9] early A-type star Cernis 52 (R.A 03 43 01; Dec +31 58 10; Cernis 1993 ) lies in the line of sight of the Perseus molecular complex which is located at a distance of about 240 pc. The star is a likely member of the very young IC 348 cluster, about 1 degree in projection away from its core (González-Hernández et al. 2009). This line of sight towards Perseus is remarkable because of the anomalous microwave emission detected by Watson et al (2005) in the frequency range 10-60 GHz. According to recent data, this anomalous emission reaches a maximum in the line of sight of Cernis 52 (Tibbs et al. 2010). This new microwave emission process cannot be explained by classical mechanisms as synchrotron, free-free or thermal emission from dust particles, however it is spatially correlated with the distribution of dust traced by IRAS images.

Draine and Lazarian (1998) postulated that the anomalous microwave emission could be due to electric dipole radiation of rapidly spinning small interstellar carbon based molecules, as for example polycyclic aromatic hydrocarbons (PAHs) (see also Iglesias-Groth 2005 for the potential contribution of hydrogenated forms of fullerenes). The recent detection of optical bands in the spectrum of Cernis 52 which

are consistent with transitions of the naphthalene  $C_{10}H_8^+$  and anthracene  $C_{14}H_{10}^+$  cations (Iglesias-Groth et al 2008, 2010) add support to this PAH hypothesis and call for a more extensive study of the physical and chemical conditions of the intervening material. Interstellar CH,  $CH^+$  have also been detected toward Cernis 52 with high column densities suggesting that the  $H_2$  column density in the intervening cloud is also high (Iglesias-Groth et al. 2010). CH is empirically correlated with  $C_2$  in diffuse and translucent molecular clouds (see e.g. van Dishoeck & Black 1989, Federman et al. 1994, Gredel 1999) thus a high column density of  $C_2$  in the intervening cloud may be expected. The basic chemical processes which lead to the formation of diatomic carbon bearing species were reviewed by Federman & Huntress (1989) and the dominant  $C_2$  formation path is  $C^+ + CH \rightarrow C_2^+ + H$ .

We report here the detection of several interstellar absorption lines of the simplest multicarbon molecule  $C_2$  toward Cernis 52 and the study of physical parameters such as gas-kinetic temperatures and particle densities in the intervening cloud. We identify many weak absorption lines of  $C_2$  leading to the estimation of column densities for levels  $J'' < 12$ . The theory of  $C_2$  excitation developed by Chaffee et al. (1980) and van Dishoeck & Black (1982) has been considered by a variety of authors in their analysis of interstellar  $C_2$  lines (see e.g. Hobbs 1981, Gredel 1999, Gredel et

\* E-mail: sigroth@iac.es

al 2001, Sonnentrucker et al. 2007, Kaźmierczak et al. 2010) to derive densities and temperatures in diffuse and translucent molecular clouds. We use the van Dishoeck & Black formalism to infer the C<sub>2</sub> total abundance, the kinetic temperature and the density of the gas in the intervening cloud. We also report the detection of an absorption feature in the spectrum of Cernis 52 which can be ascribed to the 4051.6 Å band of C<sub>3</sub>.

## 2 OBSERVATIONS AND DATA REDUCTION

Interstellar absorption lines which arise from the (2,0) and (3,0) bands of the C<sub>2</sub> Phillips system around 8765 and 7720 Å, respectively, were searched toward star Cernis 52. The observations were carried out in November 2008 using the High Resolution Spectrograph (HRS) of the 9.2m Hobby-Eberly Telescope (HET) at McDonald Observatory (Texas, USA). Exposures of the star's spectrum were obtained on each of four nights (November 4, 7, 9 and 29) at a resolving power R=40000. In all, 15 exposures lasting 20 minutes each were obtained and were subsequently combined during data reduction. Fast rotating stars were also observed with the same instrument on the same nights to allow removal of telluric lines and correction of the instrumental response. The data were reduced using IRAF and wavelength calibrated using ThAr lamps. The dispersion of the re-binned linear data was 96 mÅ/pixel. The fiber used to feed HRS led to a spectral resolution of 0.25 Å in the spectral regions of interest. The accuracy of the wavelength calibration of each order was better than 10 mÅ as shown by measurements of the wavelengths of telluric lines recorded in various echelle orders. After wavelength calibration, the Cernis 52 spectra were corrected for telluric line contamination and possible instrumental effects dividing each individual spectrum by the featureless spectrum of a much brighter, hot and fast rotating star in a nearby line of sight observed with the same instrument configuration. Individual spectra were then combined to improve S/N. The final spectrum achieved S/N ≥ 300 per pixel.

Cernis 52 is embedded in a cloud responsible for significant visible extinction and the presence in the spectrum of molecular absorption bands caused by the intervening interstellar material is therefore expected. Figures 1 and 2 show interstellar absorption lines which arise from the (2,0) and (3,0) bands of the C<sub>2</sub> A<sup>1</sup>Π<sub>u</sub> - X<sup>1</sup>Σ<sup>+</sup><sub>g</sub> Phillips System, around 8765 Å and 7720 Å, respectively. We identified and measured absorption lines (P,Q and R branches) in bands (2,0) 8750-8849 Å and some of (3,0) 7714-7793 Å. The equivalent widths in the final normalized spectra were measured by fitting a Gaussian profile to each absorption line using the IRAF task SPLOT. In the case of unresolved line blends, such as the (2,0) R(10)+R(2) blend, we used the deblending option offered by the same routine to determine the equivalent width of each component. The equivalent widths with errors for all the measured interstellar lines of C<sub>2</sub> are listed in Table 1. The observational uncertainties in the equivalent widths are typically ±1 mÅ, except for those lines marked as blends which have errors of ~2 mÅ. The table lists rest wavelengths in air obtained from the wavenumbers in vacuum of Chauville, Maillard and Mantz (1977) and converted to air wavelengths using Birch & Downs (1993).

## 3 RESULTS AND ANALYSIS

### 3.1 Molecular parameters

The measured equivalent widths  $W_\lambda$  of the C<sub>2</sub> lines were converted into column densities for individual rotational levels  $N(J'')$  assuming that the absorption lines are optically thin (i.e. that the absorption lines are on the linear part of the curve of growth). This approximation is accurate to better than 10 per cent for  $W_\lambda < 10$  mÅ and Doppler widths  $b > 1$  km s<sup>-1</sup> (Stromgren 1948). We used the following equation with  $W_\lambda$  in units of Å and  $N$  in units of cm<sup>-2</sup>

$$N(J'') = 1.13 \times 10^{20} W_\lambda / (f_{J',J''} \lambda^2) \quad (1)$$

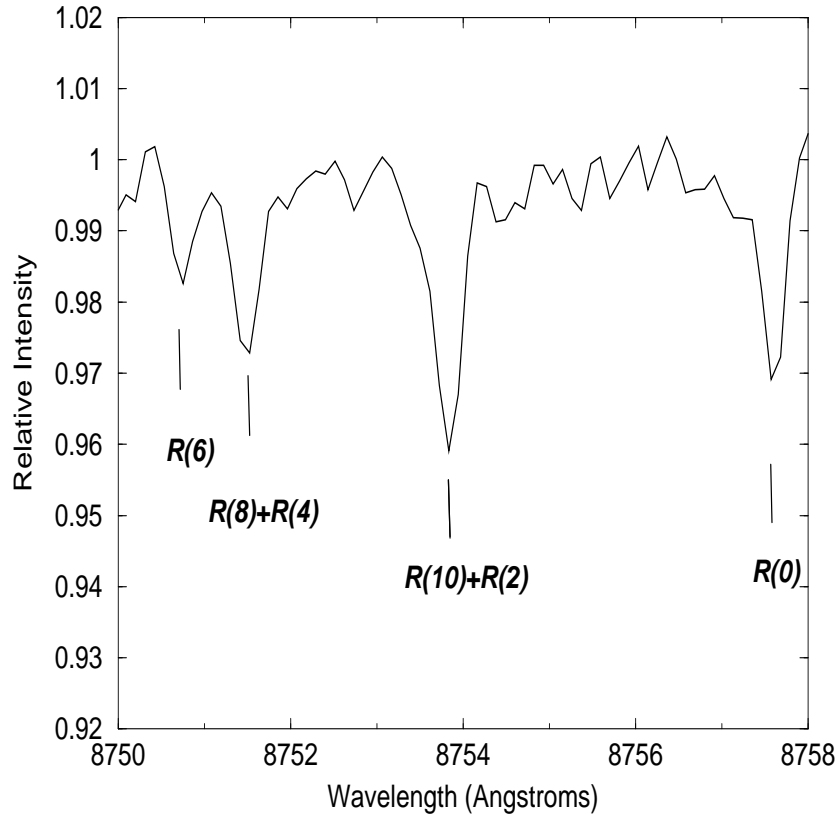
where  $\lambda$  is wavelength and  $f_{J',J''}$  is the absorption oscillator strength.

Line oscillator strengths  $f_{J',J''}$  were calculated from the (2,0) band oscillator strength  $f_{20}$  from the relation  $f_{J',J''} = f_{20} (\nu_{J',J''} / \nu_{band}) S_{J',J''} / (2(2J'' + 1))$ , and Hönl-London rotational line intensity factors  $S_{J',J''}$  of ( $J'' + 2$ ), ( $2J'' + 1$ ), and ( $J'' - 1$ ) for the R, Q, and P lines, respectively. The general formulae for the Hönl-London factors (Herzberg 1950) are simplified to the former values and normalized such that for each  $J''$  the sum  $\sum_{J'} S_{J',J''} / g(2J'' + 1) = 1$ , where  $g=2$  is the value of the ratio of electronic degeneracy factor for the C<sub>2</sub> A-X system. Here  $\nu_{band}$  is the wavenumber of the band, equal to 11413.91 cm<sup>-1</sup> for the Phillips (2-0) band. For the absorption oscillator strength of the (2-0) Phillips band we used the value  $f_{20} = 1.36 (\pm 0.15) \times 10^{-3}$  measured by Erman and Iwamae (1995) which compares well with  $1.44 \times 10^{-3}$  as obtained from an ab initio calculation by van Dishoeck (1983) and with the value  $f_{20} = 1.2 \times 10^{-3}$  suggested by Lambert et al. (1995). We infer the band oscillator strength for the (3,0) band from  $f_{20}$  using the theoretical ratio of  $f_{20}/f_{30} = 2.2$  (van Dishoeck & Black 1982).

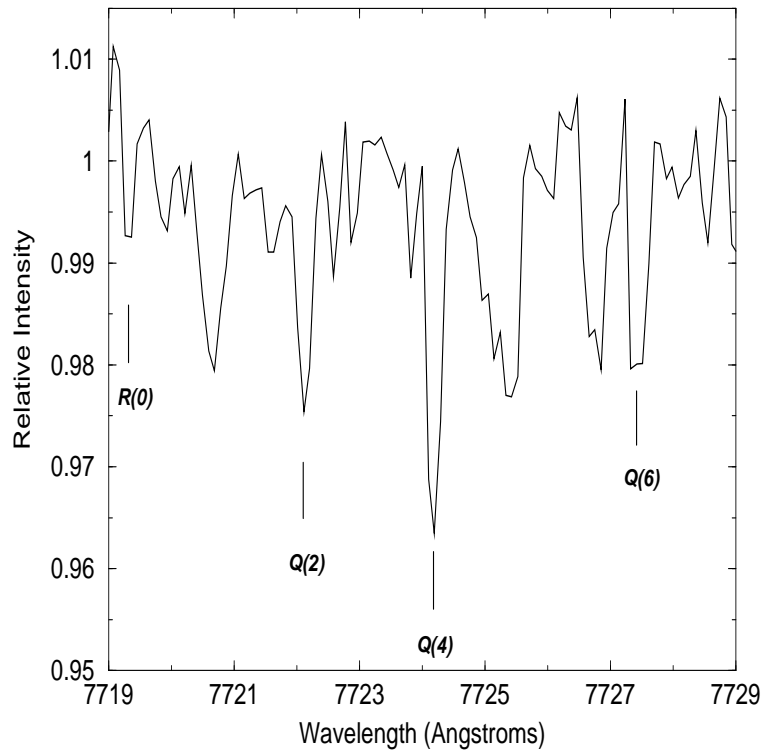
#### 3.1.1 Column densities and Rotational excitation of C<sub>2</sub>

As discussed by Gredel et al. (2001) a curve of growth analysis shows that for a typical value of  $b = 1$  km s<sup>-1</sup> the C<sub>2</sub> lines suffer from saturation for  $W_\lambda > 15$  mÅ. All our C<sub>2</sub> lines are weaker than this value and therefore we have ignored saturation corrections. The derived column densities for each rotational level  $N(J'')$  are listed in Table 1 with their uncertainties. An independent check on the reliability of the results can be made by a comparison of the column densities derived from the P, Q and R lines which arise from the same lower level  $J''$ . Because of the smaller oscillator strength of P lines they proved very difficult to measure. Thus, the empirical uncertainties in  $N(J'')$  of order 20 % are obtained by comparing for each  $J''$  the values obtained from R(J) and Q(J) lines.

In order to obtain average column densities  $\langle N(J'') \rangle$  in rotational level  $J''$ , the column densities inferred from the individual measurements in the R and Q lines of the (2,0) and (3,0) bands, when available, were combined. Following van Dishoeck and Black (1982), we obtain the C<sub>2</sub> excitation diagram for Cernis 52 shown in Fig. 3 where we represent the weighted relative column densities  $-\ln [5 N(J'') / ((2J'' + 1) N(2))] / (k E(J''))$  versus excitation energy  $E(J'')$  of rotational level  $J''$  ( $k$  is the Boltzmann constant). Rotation excitation temperatures were obtained from a linear fit to the logarithm of the column densities of the two, three and four lowest rotational



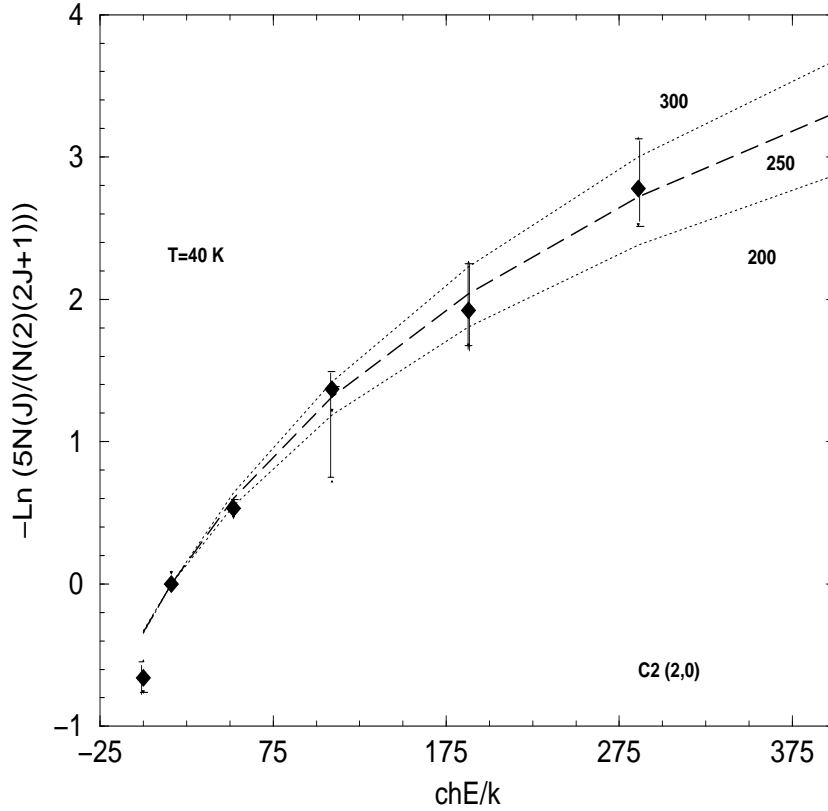
**Figure 1.** Fig. 1. Spectrum covering the (2,0) band of the  $C_2$  Phillips System towards Cernis 52. Detected rotational lines are identified.



**Figure 2.** Spectrum covering the (3,0) band of the  $C_2$  Phillips System towards Cernis 52. Detected rotational lines are identified

**Table 1.** Summary of C<sub>2</sub> lines toward Cenis 52. (a-blend line).

| Molecule | Band      | Line       | $\lambda_{air}(\text{\AA})$ | $W_{\lambda}(\text{m\AA})$                | $N(J'') (10^{13}\text{cm}^{-2})$ |
|----------|-----------|------------|-----------------------------|---|----------------------------------|
| C2       | A-X (3-0) | R(0)       | 7719.33                     | 3(1)                                      | 0.91 (0.3)                       |
|          |           | R(2)       | 7716.53                     | 5(2)                                      | 3.56 (1.4)                       |
|          |           | R(6)+R(4)  | 7714.58+7714.95             | 5(2) <sup>a</sup> +3(2) <sup>a</sup>      | 1.98(0.8)+2.78 (1.8)             |
|          |           | R(10)      | 7717.47                     | 1.5(1)                                    | 1.6 (1)                          |
|          |           | Q(2)       | 7722.10                     | 4.3(1)                                    | 2.04 (0.5)                       |
|          |           | Q(4)       | 7724.22                     | 6.5(1)                                    | 2.69 (0.5)                       |
| C2       | A-X (2-0) | Q(6)       | 7727.56                     | 3(1)                                      | 1.45 (0.5)                       |
|          |           | R(6)       | 8750.85                     | 4.3(0.5)                                  | 1.51 (0.4)                       |
|          |           | R(8)+R(4)  | 8751.49+8751.68             | 3(1) <sup>a</sup> +6.5(1) <sup>a</sup>    | 1.11 (0.4) +2.13 (0.3)           |
|          |           | R(10)+R(2) | 8753.58+8753.95             | 2.4(1) <sup>a</sup> +14.8(1) <sup>a</sup> | 0.91(0.4)+4.04 (0.6)             |
|          |           | R(0)       | 8757.69                     | 8.4(1)                                    | 0.91 (0.1)                       |
|          |           | Q(2)       | 8761.19                     | 10(1)                                     | 2.16 (0.2)                       |
|          |           | Q(4)       | 8763.75                     | 11.9(1)                                   | 2.57 (0.2)                       |
|          |           | P(2)       | 8766.03                     | 3 <sup>a</sup>                            |                                  |
|          |           | Q(6)       | 8767.76                     | 7.4 <sup>a</sup>                          | 1.60 (0.4)                       |
|          |           | Q(8)+P(4)  | 8773.22+8773.43             | 4(2) <sup>a</sup> +5(2) <sup>a</sup>      | 1.29(0.6)+3.00(0.5)              |
|          |           | Q(10)      | 8780.14                     | 2.5(1)                                    | 0.54 (0.2)                       |
|          |           | Q(12)      | 8788.56                     | 3 (1)                                     | 0.64 (0.2)                       |

**Figure 3.** C<sub>2</sub> excitation diagram for Cenis 52, with observed relative rotational populations with respect to that of the  $J''=2$  level as function of the excitation energy  $E(J'')$ . Filled diamonds correspond to individual line detections. The  $1\sigma$  error bars are indicated. The theoretical populations (dotted and dashed lines) at a kinetic temperature  $T = 34$  K are shown for comparison at several densities  $n$  (see text). The dot-dashed line indicates the thermal distribution at  $T=34$  K.

levels starting from  $J''=0$  and result  $T_{02}=34$  K,  $T_{04}=39$  K and  $T_{06}=49$  K, respectively.

As described by van Dishoeck and Black (1982), in general the populations of all rotational levels cannot be characterized by a single rotational temperature, the detailed behaviour of the rotational excitation temperature depends on the gas kinetic temperature  $T_{kin}$ , on the intensity of the interstellar radiation field  $I$  and on the collisional rate  $n\sigma_0$

(the number density of collision partners  $n = n(\text{H}) + n(\text{H}_2)$  times the cross section,  $\sigma_0$ , for collision induced transitions for level  $J''$  to rotational level  $(J'' - 2)$ ). To interpret the excitation diagram of Fig. 3 we assume the same  $\sigma_0 = 2 \times 10^{-16} \text{ cm}^2$  and the same intensity of the interstellar radiation field than van Dishoeck and Black (1982) and adjusted for the differences with respect their adopted  $f$  values. We infer from these models an excitation temperature

of  $34 \pm 10$  K and for the effective density of collision partners  $n = 300 \pm 80 \text{ cm}^{-3}$  (see Fig. 3). We checked this result using the code made available by B. Mc Call at the web site <http://dib.uiuc.edu/c2/>. We generated a grid of models for gas kinetic temperatures ranging from 10 to 1000 K, with a step of 1 K and a range of particle densities from  $n = 50$  to  $2000 \text{ cm}^{-3}$  with a step of  $50 \text{ cm}^{-3}$ . The results were scaled to the  $f$ -values adopted above (a factor 1.36 higher than in the code by Mc Call) for the (2,0) series and we took for comparison the weighted mean of the column densities  $N(J)$  inferred from the (2,0) series of lines. Then, we determined from the best figure of merit (obtained from the minimum difference between predicted and observed values) the most likely values for  $T$  and  $n$ . The best fit was found at  $T = 40 \pm 10$  K and  $n = 250 \pm 50 \text{ cm}^{-3}$  in very good agreement with our previous independent analysis.

Total observed column densities were derived from the sum  $\sum_{J''} N(J'')$  over the observed rotational levels of each individual band, resulting  $N_{obs} = (9.2 \pm 1.4) \times 10^{13} \text{ cm}^{-2}$  and  $(9.8 \pm 1.5) \times 10^{13} \text{ cm}^{-2}$  for the (2,0) and (3,0) bands, respectively. The combination leads to  $N_{obs} = (9.5 \pm 1.2) \times 10^{13} \text{ cm}^{-2}$ . The total  $C_2$  column density, defined as the sum of the mean column densities of the observed levels and of the contribution of the unobserved levels estimated from the theoretical model characterized by the best-fitting parameters results  $N_{tot} = (10.5 \pm 1.2) \times 10^{13} \text{ cm}^{-2}$ .

Heliocentric velocities for individual interstellar absorption lines of  $C_2$  were determined from the final combined spectrum obtained each of the four days that Cernis 52 was observed. Typically, the three or four most intense unblended lines for each band were used. We found  $14.9 \pm 1.0$  and  $12.7 \pm 1.2 \text{ km s}^{-1}$  as average values of the heliocentric velocities of the lines measured for the (2,0) and (3,0) bands, respectively. The error was obtained as the rms of the measurements. We find consistent results among the two bands and finally combine them to obtain an average heliocentric velocity of  $v_{hel} = 13.8 \pm 0.9 \text{ km s}^{-1}$  as best estimate from the detected interstellar  $C_2$  lines. It appears, at this spectral resolution, that  $C_2$  lines rise in a single velocity component. The  $C_2$  lines and the K I line (see below) display the same heliocentric velocity within the uncertainties of our measurements.

### 3.2 Interstellar Potassium

The K I 7664 and 7698 Å absorption lines are also present in our spectra of Cernis 52. The K I 7698 line is well separated from a telluric  $O_2$  absorption line but the K I 7664 line is not. The equivalent width of the K I 7698 Å line is  $153 \pm 3 \text{ mÅ}$ . We have obtained heliocentric velocities for this K I line from the available set of spectra resulting a final mean value of  $13.7 \pm 0.4 \text{ km s}^{-1}$  where the error is obtained from the dispersion of the measurements obtained in different days. The heliocentric velocity agrees well with those of  $C_2$  above and CH,  $CH^+$  measured by Iglesias-Groth et al. (2010). Using the atomic parameters of Morton (1991), we infer  $N(K) = 1.4 \times 10^{12} \text{ cm}^{-2}$  towards Cernis 52.

## 4 DISCUSSION

Out of 37 lines of sight towards translucent molecular clouds investigated by van Dishoeck and Black (1989, see their table 4) 19 present  $E(B-V)$  higher than Cernis 52 but only 4 show  $C_2$  column densities higher than this star. Remarkably, the column density of Cernis 52 is about 2 times larger than the average value observed toward stars with similar  $E(B-V)$ . Out of 12 lines of sight investigated by Gredel (1999) with  $E(B-V)$  higher than Cernis 52 only 2 showed  $C_2$  column densities comparable or higher than Cernis 52. The  $C_2$  column density derived for Cernis 52 is one of the largest so far observed in translucent molecular clouds. Although its value is not as large as the one toward the much more heavily reddened star Cygnus OB2 No. 12 with  $E(B-V) = 3.31$  reported to be  $20 \times 10^{13} \text{ cm}^{-2}$  (Gredel et al. 2001). It is however comparable to the highest values reported for the stars in Gredel (1999) where star HD 172028 displays one of the highest  $C_2$  column densities ( $N(C_2) = (11 \pm 0.5) \times 10^{13} \text{ cm}^{-2}$ ) comparable to our measurement for Cernis 52. HD 172028 displays moderate extinction ( $A_V = 2.3$ ) as and Gredel determines a kinetic temperature of 30 K and density of  $300 \pm 100 \text{ cm}^{-3}$  for the intervening cloud, both values are very similar to those found for the cloud in the line of sight of Cernis 52.

The heliocentric velocities of  $C_2$  and CH in Cernis 52 coincide so it is very likely that both molecules co-exist to a large extent in the same region. The  $C_2$  and CH column densities of translucent molecular clouds are empirically well correlated and appear to follow the relationship  $\log N(C_2) = 0.85 \log N(CH) + 2.2$  (van Dishoeck & Black 1989). Theoretical reasons for this correlation are discussed by Federman et al. (1994). Using the previous relationship and the CH column density  $N(CH) = 20 (\pm 2) \times 10^{13} \text{ cm}^{-2}$  of Iglesias-Groth et al. (2010) we expected a column density of  $C_2$  of  $\sim 22 \times 10^{13} \text{ cm}^{-2}$ . This is about a factor 2 higher than our measurement, however the column density of CH derived for Cernis 52 is significantly affected by saturation of the observed absorption line and the applied correction may have led to an overestimation of the abundance by some 50%. With this consideration in mind and using the relation  $N(H_2) = 2.6 \times 10^7 N(CH)$  of Somerville & Smith (1989) we estimate a column density of  $N(H_2) = 5 \times 10^{21} \text{ cm}^{-2}$ , but cannot discard a value a factor two lower because of the saturation correction just mentioned. The fractional abundance  $f(C_2) = N(C_2)/N(H)$ , that is  $f(C_2) \sim N(C_2)/2N(H_2) \sim N(C_2)/2N(H)$  is  $\sim 1 \times 10^{-8}$  which compares well with values  $0.5\text{-}1.5 \times 10^{-8}$  obtained by Gredel (1999) toward stars in the association surrounding NGC 2439, in Vela OB 1 and in Cen OB1 in spite of generally higher gas kinetic temperatures and densities towards these lines of sight.

Observations of the  $A^1\Pi_u - X^1\Sigma^+_g$  transition of  $C_3$  at  $4051.6 \text{ Å}$  in translucent sight lines have been reported by Oka et al. (2003) and Ádámkóvics et al. (2003). The observed  $C_3$  column densities range from  $10^{12}$  to  $10^{13} \text{ cm}^{-2}$  and are well correlated with the corresponding  $C_2$  columns with a ratio  $N(C_2)/N(C_3) \sim 40$ . The observed strong correlation suggests that  $C_3$  and  $C_2$  are involved in the same chain of chemical reactions. As discussed by Oka et al.,  $C_3$  formation may result from  $C_2$  by photoionization, ion neutral reactions and dissociative recombinations. The spectral range of our HET spectra do not cover this transition, but

fortunately, the spectra of Cernis 52 obtained with the blue arm of ISIS at the 4.2m William Herschel Telescope (described in Iglesias-Groth et al. 2010) do include the relevant spectral range to search for this transition. We report the detection of an absorption feature with an equivalent width of  $W_\lambda = 6 \pm 1.5 \text{ m\AA}$  fully consistent in wavelength with the transition from  $C_3$ . The feature presents a weaker blend on the blue wing whose origin can be understood looking at the simulated spectra by Haffner and Meyer (1995) for the 4051.6 band of  $C_3$  in clouds of  $T=40 \text{ K}$  which fits well the conditions of our cloud, or simulations for a larger range of temperatures by Ádámkóvics et al. (2003). The blue line of the blend appears to be caused by the pileup of rovibronic transitions of the first lines of the R series in the wavelength range 4050-4051 Å. The main feature is due to the stronger lines of the Q series in the range 4051-4052 Å. Our equivalent width would mostly correspond to the pileup of these Q-branch lines. The resolving power of the WHT spectra is not sufficient to measure individual rotational lines and therefore does not allow us to derive the temperature of the cloud from  $C_3$  which would have provided an interesting comparison with the results derived from  $C_2$ . Our data provides however a preliminary estimate of the column density for  $C_3$ . Adopting the simplest assumption of a one-temperature rotational distribution, following the arguments given by Oka et al. (2003) (we multiply by a factor 2 the right term of the  $W_\lambda - N$  expression in Section 3.1) and using their oscillator strength of  $f=0.016$  we derive  $N(C_3) = (5.2 \pm 1.3) \times 10^{12} \text{ cm}^{-2}$  and a ratio of  $N(C_2) / N(C_3) = 20_{-6}^{+10}$  which is comparable to those derived in the above papers for other lines of sight.

Models of quiescent translucent molecular clouds are presented by van Dishoeck and Black (1988) for a range of total visual extinction  $A_V$  (1-5 mag), densities ( $500\text{-}1000 \text{ cm}^{-3}$ ) and temperatures (15-40 K). Computed column densities for several species (CH,  $C_2$ , CN, CO, etc...) in these models can also be found in van Dishoeck & Black (1988) which may help to predict the abundance of other species in the intervening cloud and prepare observing programmes for an extensive characterization. The constraints on density ( $250 \pm 50 \text{ cm}^{-3}$ ) and gas kinetic temperature ( $40 \pm 10 \text{ K}$ ) that we have obtained provide already valuable information for the modelling of the anomalous microwave emission in the Perseus complex. The models computed by Iglesias-Groth (2005) to explain the spectral energy distribution of electric dipole radiation from hydrogenated carbon particles in this light of sight should be revised accordingly. However, we recall here that to infer the density of the cloud a major assumption was made on the value of the intensity of the radiation field in the near infrared, and since the excitation temperature curves are degenerated versus the ratio of the density to the intensity field, we would still require an independent determination of the radiation field instead of an assumption on its value, to determine proper abundances. For instance, the strength of the radiation field was inferred to be enhanced by a factor of 3-5 in  $\zeta$  Oph and other diffuse clouds with similar kinetic temperatures (van Dishoeck & Black 1988). The incident radiation field in the translucent cloud may also be enhanced because of the presence of Cernis 52. For the moment, with the limited number of molecular species so far observed toward Cernis 52, we cannot constrain the parameter of the radiation field any

further. However, plausible models for the Cernis 52 cloud predict significant column densities for a variety of atomic and molecular species which may be observed in the near future (H,  $H_3^+$ ,  $C_2H$ ,  $C_2H_2$ , OH,  $H_2O$ , NH,  $CH_2$ , etc.) and could in principle provide much better constraints on the basic parameters of the model. Simple steady state chemical kinetics (Oka et al.) indicate that the neutral molecules  $C_2$ ,  $C_2H$ ,  $C_2H_2$  and  $C_3$  are more abundant than the ionic species by at least 2 orders of magnitude.

#### 4.1 Comparison with other lines of sight in Perseus

The diffuse clouds toward  $\zeta$  Per and *omi* Per have been extensively studied since early work on interstellar  $C_2$  (Black, Hartquist and Dalgarno 1978, Hobbs 1979, Chaffee et al. 1980, van Dishoeck & Black 1989). These two stars are located in the Perseus molecular complex, but in lines of sight where anomalous microwave emission is not detected, if this emission exists it is definitely much weaker than in the line of sight of Cernis 52. According to van Dishoeck & Black (1982) the molecular core of the  $\zeta$  Per cloud would have  $n=150 \text{ cm}^{-3}$ ,  $T=45 \text{ K}$  and  $I \sim 0.7$  and the column density of  $C_2$  would be  $N(C_2) = 1.6 \times 10^{13} \text{ cm}^{-2}$  which compares well with the predictions in the early model by Black et al. (1978). A recent summary of results on gas kinetic temperatures and densities for these and other diffuse and translucent clouds can be found in Sonnentrucker et al. (2007). The physical conditions in these two clouds are apparently not very different to those estimated for Cernis 52 but the extinction is 3 times higher and the abundance of  $C_2$  and CH are  $\sim 10$  times higher than in  $\zeta$  and *omi* Per. It is possible that reactions causing destruction ( $C_2 + H_2 \rightarrow C_2H + H$ ) and production ( $C_2H + h\nu \rightarrow C_2 + H$ ) of  $C_2$  work at very different rates at the lower temperature of the Cernis 52 cloud. A search for lines of  $C_2H$  in the optical or radio would provide valuable insight on the reasons for the much higher column density of  $C_2$  in Cernis 52 and will contribute to a better understanding of the physical conditions there and in particular of the processes involved in the formation of naphthalene and anthracene cations in the intervening cloud (Iglesias-Groth et al. 2008, 2010).

## 5 CONCLUSIONS

We have presented observations of interstellar absorption lines of  $C_2$  toward Cernis 52. We have identified six rotational lines of the (2,0) and five rotational lines of the (3,0) Phillips system. The population distribution in the lowest rotational levels indicates a rotational excitation temperature of  $T_{rot} = 34 \pm 12 \text{ K}$ . A detailed study of the level population leads to a best fit gas kinetic temperature  $T = 40 \pm 10 \text{ K}$  and particle density  $n = 250 \pm 50 \text{ cm}^{-3}$  for the molecular gas in the intervening cloud. We obtain a total  $C_2$  column density of  $(10.5 \pm 1.2) \times 10^{13} \text{ cm}^{-2}$ . We also report a tentative detection of an interstellar absorption feature at the wavelength (4051.6 Å) expected for an unresolved blend of the strongest Q-branch lines arising from the ground vibrational state of the  $C_3$   $A^1\Pi_u - X^1\Sigma_g^+$  electronic transition and derive from this a column density for  $C_3$  of  $(5.2 \pm 1.3)$

$\times 10^{12} \text{ cm}^{-2}$ . The ratio C<sub>2</sub>/C<sub>3</sub> compares well with those reported in the literature on translucent clouds (Oka et al. 2003). Higher resolution, higher S/N data will be required to confirm the C<sub>3</sub> detection and to determine the weak rotational structure of the band which could be used as an independent diagnostic of the cloud's kinetic gas temperature. In addition, it is worth to search for longer multicarbon chains (C<sub>4</sub>, C<sub>5</sub>,... C<sub>18</sub>) in this rather carbon-rich sight line. The growth of carbon chains from C<sub>2</sub> and C<sub>3</sub> via C<sup>+</sup> association followed by H abstraction and recombination may be fast after C<sub>4</sub> (Freed et al. 1982). This line of sight is well suited to carry out such studies which will provide insight on carbon chemistry.

In the intervening cloud toward Cernis 52, C<sub>2</sub> forms dominantly in cool material at gas kinetic temperatures of  $40 \pm 10 \text{ K}$ . The C<sub>2</sub> and CH column densities are apparently both high and their relative value follow the expectations from theoretical models of translucent molecular clouds and the well established empirical relationship for this two species. The C<sub>2</sub> molecules mainly probe the dense cold core of the cloud, measurements of column densities of H, H<sub>2</sub> in various rotational levels and C in various fine structure levels would be worth to model in detail the intervening cloud and gain insight on the physical processes causing the anomalous microwave emission, it is important to obtain also information on a possible warmer less dense envelope. Observations of C<sub>2</sub>H may help to explain the high content of C<sub>2</sub>. This molecule may provide pathways to the formation of long-chain carbon molecules and is likely that a high content may have also favoured the formation of PAHs to a detectable level. Additional observations may establish the chemistry of the cloud and the role that a high content of C<sub>2</sub> and CH could have on the formation of PAHs.

## ACKNOWLEDGEMENTS

I thank D.L. Lambert and R. Rebolo for useful comments on this paper. This work was partially supported by grant AYA-2007-64748 from the Spanish Ministry of Science and Innovation.

## REFERENCES

- Adámkóvics M., Blake, G.A. & McCall, B.J. 2003, ApJ, 595, 235
- Bakker, E. J., Waters, L. B. F. M., Lamers, H. J. G. L. M., Trams, N. R. & van der Wolf, F. L. A. 1996, A&A, 310, 893
- Black, J. H., Hartquist, T. W. & Dalgarno, A. 1978, ApJ 224, 448
- Birch, K. P., & Downs, M. J. 1993, Metrologia, 30, 155.
- Chaffee, F. H., Jr., Lutz, B. L., Black, J. H., Vanden Bout, P. A. & Snell, R. L. 1980, ApJ, 236, 474
- Chaffee, F. H., Jr. & White, R. E. 1981, BAAS, 13, 509
- Cernis, K. 1993, Baltic Astronomy 2, 214
- Chauville, J. Maillard, J.P., Mantz, A.W. 1977, J.Mol.Spect. 68, 399
- Draine, B.T. & Lazarian, A. 1998a, ApJ, 494, L19
- Davis, S. P., Shortenhaus, D., Stark, G., et al. 1986, ApJ, 303, 892
- Federman, S. R. & Huntress, W. T., Jr. 1989, ApJ 338, 140
- Federman, S. R., Strom, C. J., Lambert, D. L., Cardelli, Jason A., Smith, V. V. & Joseph, C. L. 1994, ApJ 424, 772
- Freed, K.F., Oka, T. & Suzuki, H. 1982, ApJ, 263, 718
- González Hernández, J.I., Iglesias-Groth, S., Rebolo, R., García-Hernández, D.A., Manchado, A. & Lambert, D.L. 2009, ApJ, 706, 866
- Gredel, R. 1999, A&A, 351, 657
- Gredel, R., Black, J.H. & Yan, M. 2001, A&A, 375, 553
- Herzberg, G., "Molecular Spectra and Molecular Structure, I. Spectra of Diatomic Molecules" 1950
- Haffner, L.M. & Meyer, D.M. 1995, ApJ 453, 450
- Hildebrandt, S. R., Rebolo, R., Rubio-Martín, J.A., Watson, R.A., Gutiérrez, C.M., Hoyland, R.J. & Battistelli, E.S. 2007, MNRAS 382, 594
- Hobbs, L. M. 1979, ApJ 232, L175
- Hobbs, L. M. 1981, ApJ 243, 485
- Hobbs, L. M., York, D. G., Snow, T. P., Oka, T., Thorburn, J.A.; Bishof, M., Friedman, S. D. & McCall, B. J. et al. 2008, ApJ 680, 1256
- Iglesias-Groth, S. 2005, ApJ 632, L25
- Iglesias-Groth, S. 2006, MNRAS 368, 1925
- Iglesias-Groth, S., Manchado, A., García-Hernández, A., González Hernández, J.I. & Lambert, D. 2008, ApJ 685, L55
- Iglesias-Groth, S., Manchado, A., Rebolo, R., Gonzalez Hernandez, J. I., Garcia-Hernandez, D. A. & Lambert, D.L. 2010, arXiv1005.4388
- Kaźmierczak, M. Schmidt M.R., Bondar, A. & Krelowski J. 2009, MNRAS 2009
- Kaczmarczyk, G. 2000, MNRAS 316, 875
- Lambert, David L., Sheffer, Yaron & Federman, S. R. 1995, ApJ 438, 740
- Morton, D.C. 1991, ApJS. 77, 119
- Oka, T., Thorburn, J.A., McCall, B.J., Friedman, S.D., Hobbs, L.M., Sonnentrucker, P., Wely, D.E. & York D.G. 2003, ApJ, 582, 823
- Sonnentrucker, P., Welty D. E., Thorburn J.A., York D.G., 2007, ApJS, 168, 58
- Somerville, W.B., Smith C.A., 1989, MNRAS 238, 559
- Stroömgren & Bengt, 1948, ApJ 108, 242
- Tibbs C. et al. 2010, MNRAS 402, 1969
- van Dishoeck, E. F. & Black, J. H. 1982, ApJ, 258, 533
- van Dishoeck, E.F. 1983, Chem. Phys., Vol. 77, No. 2, p. 277 - 286
- van Dishoeck, E. F. & Zeeuw, T. 1984, MNRAS 206, 383
- van Dishoeck, E. F. & Black, J. H. 1988, ApJ 334, 771
- van Dishoeck, E. F. & Black, J. H. 1989, ApJ 340, 273
- Watson, R.A., Rebolo, R. et. al. 2005, ApJ 624, L89
- Erman, P., & Iwamae, A. 1995, ApJ, 450, L31